[논 문] 한국재료학회지
Kor. J. Mater. Res.
Vol. 19, No. 2 (2009)

DOI: 10.3740/MRSK.2009.19.2.085

Hydroxyapatite-Zirconia Composite Thin Films Showing Improved Mechanical Properties and Bioactivity

Min-Seok Kim, Jae-Jun Ryu* and Yun-Mo Sung†

Department of Materials Science and Engineering, Korea University, Seoul 136-713, South Korea
*Department of Prosthodontics, Medical School, Korea University, Seoul 136-701, South Korea

(Received December 23, 2008 : Received in reviced form January 7, 2009 : Accepted January 14, 2009)

Abstract Nano-crystalline hydroxyapatite (HAp) films were formed at the Ti surface by a single-step micro-arc oxidation (MAO), and HAp-zirconia composite (HZC) films were obtained by subsequent chemical vapor deposition (CVD) of zirconia onto the HAp. Through the CVD process, zero- and one-dimensional zirconia nanostructures having tetragonal crystallinity (t-ZrO_2) were uniformly distributed and well incorporated into the HAp crystal matrix to form nanoscale composites. In particular, (t-ZrO_2) was synthesized at a very low temperature. The HZC films did not show secondary phases such as tricalcium phosphate (TCP) and tetracalcium phosphate (TTCP) at relatively high temperatures. The most likely mechanism for the formation of the t-ZrO_2 and the pure HAp at the low processing temperature was proposed to be the diffusion of Ca^{2+} ions. The HZC films showed increasing micro-Vickers hardness values with increases in the t-ZrO_2 content. The morphological features and phase compositions of the HZC films showed strong dependence on the time and temperature of the CVD process. Furthermore, they showed enhanced cell proliferation compared to the TiO_2 and HAp films most likely due to the surface structure change.

Key words hydroxyapatite, zirconium dioxide, biomaterials, MTT assay.

1. Introduction

Owing to intrinsic high specific strength and biocompatibility arising from native oxide (TiO_2) layer, Ti or Ti alloys have been widely used for dental and orthopedic prostheses.[1-3] However, they suffer from slow bone bonding due to bioinertness of the oxide layer. On the other hand, hydroxyapatite (HAp: $Ca_{10}(PO_4)_6(OH)_2$), a calcium phosphate ceramic, is a major constituent of bone and thus it shows high biocompatibility and bioactivity in a human body.[4-6] For this reason, HAp coated dental and orthopedic implants have been widely investigated because they can reduce the healing time by supporting osteointegration between implants and bones. Therefore, HAp-coated Ti or Ti alloy emerged as a substitute for the pre-existing biomaterials and so far it has been proposed as the most desirable one for dental and orthopedic prosthesis.[7-11] However, the HAp films coated at the surface of Ti or Ti alloys still show critical drawbacks of low friction resistance and brittleness especially during the implantation surgery for instance dental fixture or bone screw fitting. To overcome these critical drawbacks, HAp should be reinforced by a high hardness and high toughness phase which can overcome severe frictional conditions during the surgery. Although there exist some HAp-based biocermic composites including HAp/wollastonite,[12] HAp/phlogophite,[13] and HAp/mullite,[14] ZrO_2 incorporated HAp (HAp/ZrO_2) composites (HZCs)[15] could be the most desirable one because zirconia (ZrO_2) is biocompatible and it has superior mechanical properties compared to other reinforcing components especially when it is in tetragonal phase (t-ZrO_2). Also, ZrO_2 phase is stable with HAp and when it is well dispersed in the HAp matrix, mechanical properties of HAp such as fracture toughness and hardness can be significantly improved according to the phase composition.[16,17]

To date, a number of HAp coating techniques on titanium have been explored, and among them, plasma spray coating has mostly been highlighted for the applications.[18,19] However, using plasma spray coating, it is very difficult to obtain uniform coating and high crystallinity of the HAp phase. Due to the high-temperature melting and the subsequent rapid cooling during plasma spray coating, amorphous and/or

†Corresponding author
E-Mail : ymsung@korea.ac.kr (Y. M. Sung).

secondary phases such as tri calcium phosphate (TCP) and tetra calcium phosphate (TTCP) appear, and these phases are highly bioresorbable. On the other hand, micro-arc oxidation (MAO) has been proposed as an effective electrochemical route to form uniform and high-quality HAp film on Ti at near room temperature.[20,21] Recently, we for the first time have reported success in the single-step crystalline HAp film formation by micro-arc oxidation (MAO).[22] We have demonstrated that highly crystalline HAp films were formed at the surface of Ti without any secondary treatments. Herein, we report our extended effort to improve mechanical stability and to further increase cell proliferation rate of HAp layer formed by MAO through tailoring nanostructured HZC coating on Ti.

2. Experimental Procedure

Commercially pure titanium (Grade 2, Hyundai Titanium Co., Incheon, South Korea) plates ($10 \times 40 \times 1\ mm^3$) were MAO treated in the electrolytes containing calcium chloride ($CaCl_2$, 96.0%, Aldrich, Milwaukee, WI) and potassium phosphate monobasic (KH_2PO_4, 99.9%, Aldrich, Milwaukee, WI). During the MAO process, applied voltage and current were 320-340 V and 34-35 A, respectively.

HZCs were obtained using a chemical vapor transport process by evaporating zirconium chloride powder ($ZrCl_4$, 99%, Aldrich, Milwaukee, WI) in a quartz tube furnace. Ti plates coated with HAp by the MAO process were used as substrates. Ar and O_2 gases (99.9999%) were used as a carrier and a reactive gas, respectively. The processing temperature varied to 300, 350, 400, 450 and 500 ^oC, while the heating rate was fixed to 16 ^oC per min. Each processing temperature was maintained for 5, 10, 20, 25 and 30 min, respectively for HAp-coated samples.

The phase composition and the volume fraction of t-ZrO_2 in HZC films were investigated using low incidence angle (5^o) X-ray diffraction (XRD). And hydroxyapatite ($Ca_{10}(PO_4)_6(OH)_2$, reagent grade, Aldrich, Milwaukee, WI) and tetragonal tetragonal zirconia (t-ZrO_2, 99.0%, Aldrich, Milwaukee, WI) powders were purchased with the aim of obtaining the volume fraction of t-ZrO_2 with different treatment temperature. Field emission scanning electron microscopy (FESEM) was employed to examine microstructures of the specimens. Micro-Vickers indentation was used to evaluate hardness of HZC films with the load of 300 g.

MG63 cells [Korean Cell Line Bank (KCLB^{TM}), Seoul, Korea] were cultured in Minimum Essential Medium (MEM, Dulbecco Eagle's MEM, Biowhittaker, Belgium) supplemented with 10% fetal bovine serum in a humidified atmosphere with 5% CO_2 at 37 ^oC. The cell suspension of 3 ml was carefully plated onto each prepared specimen and the cells were allowed for 3 days to attach to the specimen. The samples coated with ZrO_2 were used for the cell culture tests. The cultured cells were detached from the specimens and they were placed in a 24-multiwell plate (Nunc^{TM}, Roskilde, Denmark). The cell viability was determined using MTT (3-(4,5-dimethy-thiazol-2-yl)-2,5-diphenyltetrazolium bromide, 5 mg/ml) assay. MTT solution of 5 μl was added to each well and MG63 cells were incubated at 37 ^oC for 4 h. At the end of the incubation period, formazan dye dissolved in 1 ml of dimetyl sulfoxide was added to each well. Light absorbance of dye was measured at a wavelength of 540 nm via UV-visible spectrophotometry (spectrophotometer: Beckman DU-650, Somerset, NJ). The attachment of cells to the specimens was analyzed by FESEM. Two samples were selected in each experimental condition and above MTT assays were conducted three times.

3. Results and discussion

The phase identification and phase composition analysis of HZC films were conducted for the ZrO_2-coated samples using XRD. As shown in Fig. 1(a), (b), they showed formation of HAp and t-ZrO_2 phases and their relative XRD peak intensities showed strong dependency on the processing time and temperature. There have been a lot of researches to show the formation of bioresorbable phases (tri-calcium phosphate: TCP and tetra-calcium phosphate: TTCP) during the MAO process.[23] On the other hand, in our samples treated at 500 ^oC no other phases related to ZrO_2 and calcium phosphates were detected except t-ZrO_2 and HAp, which would play a pivotal role in giving reliability to the HZC films for biomedical applications. From Fig. 1 (a) the relative intensity of ZrO_2 diffraction peaks increases compared to that of HAp with ZrO_2 treatment time. In addition, it is worth noticing that t-ZrO_2 phase was formed during ZrO_2 treatment. It is well known that ZrO_2 bulk materials with monoclinic phase (m-ZrO_2) are not obtainable at room temperature due to sudden failure by the large volume expansion (~10%)

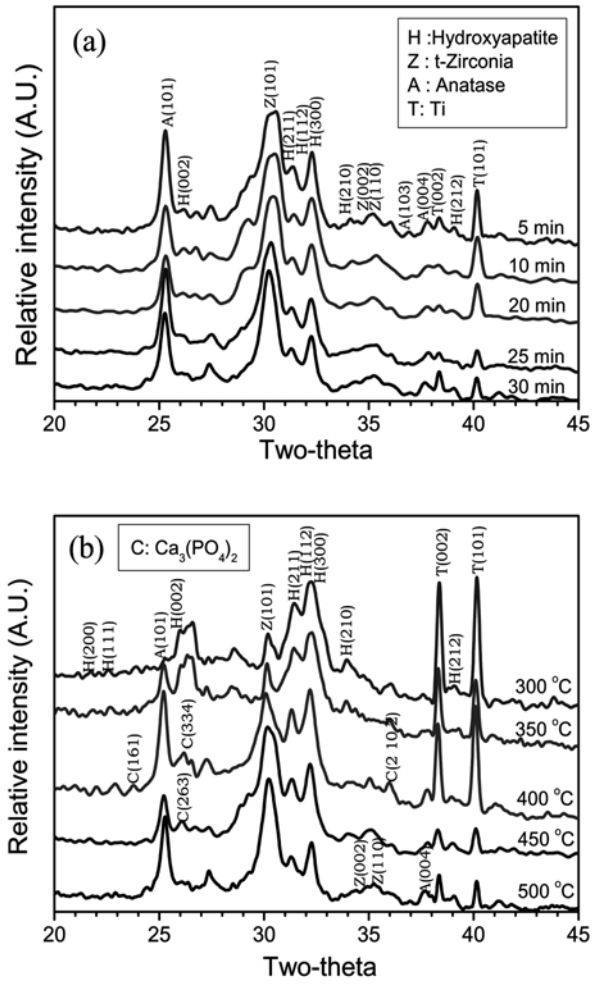

Fig. 1. (a) X-ray diffraction (XRD) patterns of ZrO_2-treated films after micro-arc oxidation (MAO) treatment. The treatment time varied with 5, 10, 20, 25, and 30 min, while the treatment temperature was fixed to 500 °C. (b) The treatment temperature varied with 300, 350, 400, 450, and 500 °C, while the treatment time was fixed to 30 min.

occurring during the transformation from high-temperature tetragonal to low-temperature monoclinic phase. Accordingly, to stabilize t-ZrO_2 phase at room temperature, ZrO_2 has been doped with yttrium, magnesium, or calcium.[24] Formation of t-ZrO_2 phase without adding dopants in our samples can be explained by the diffusion of Ca^{2+} ions from HAp layer to ZrO_2 as following[9]:

$$Ca^{2+} \xrightarrow{ZrO_2} Ca''_{Zr} + V_O^{\bullet\bullet} + O_O^x \quad (1)$$

Due to nanoscale size of ZrO_2 phase, Ca doping into ZrO_2 crystal lattices could be very easily completed.

As CVD treatment temperature increases, the relative intensity of t-ZrO_2 diffraction peaks increases compared

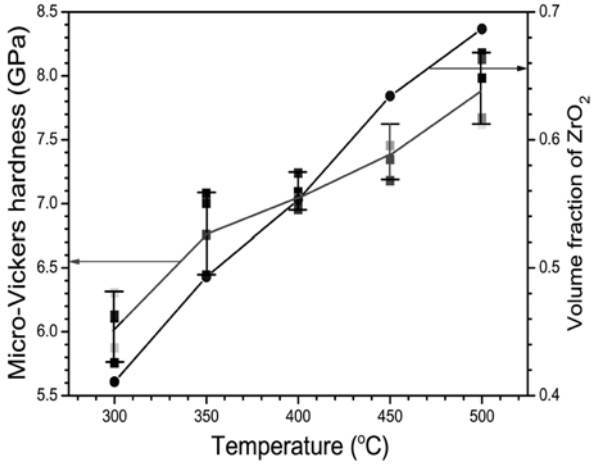

Fig. 2. The variation in the micro-Vickers hardness of hydroxyapatite-zirconia composite (HZC) films and that in the volume fraction of t-ZrO_2 with different treatment temperature.

to that of HAp as shown in Fig. 1b. Also, anatase TiO_2 peaks showed steady increase with temperature, indicating further oxidation of Ti substrates. TCP ($Ca_3(PO_4)_2$) diffraction peaks existing at around 26 ° showed the apparent intensity decrease with the treatment temperature. TCP could not be found in the ZrO_2 samples treated at 450 (d) and 500 °C (e). In spite of supplying Ca^{2+} ions to ZrO_2, the films maintain HAp phase since $CaTiO_3$ layer existing between HAp layer and Ti substrates can act as a Ca^{2+} ion reservoir.[22] The $CaTiO_3$ layer is in low crystallinity and Ca^{2+} ion diffusion to HAp layer can readily occur to meet the chemical stoichiometry of HAp. Disappearance of TCP phase in the ZrO_2 samples treated at high temperature could support our suggested mechanism of Ca^{2+} ion diffusion.

Fig. 2 shows the variation in the Vickers hardness of HZC films with different processing temperature at a fixed treatment time of 30 min. When applying the load of 300 g, the indentation size is about 26~30 μm and the penetration depth is about 9~12 μm. Therefore, it is possible to estimate the average values of hardness affected by both HAp and t-ZrO_2. The volume fraction of t-ZrO_2 was plotted together for comparison. For the purpose of confirming the relative amount of HAp and t-ZrO2 phases, the volume fraction of t-ZrO_2 (X_β) was defined as[17]

$$X_\beta = \frac{PW_\beta}{1 + (P-1)W_\beta} \quad (1)$$

where

$$W_\beta = \frac{I_{\beta(101)}}{I_{\beta(101)} + I_{H(112)}} \quad . \qquad (2)$$

Here, $I_{\beta(101)}$ and $I_{H(112)}$ are the relative XRD intensity values of t-ZrO_2 (101) and HAp (112), respectively. The coefficient of P representing the relative intensity ratio of the HAp (112) reflection to the ZrO_2 (101) reflection was determined using XRD on the mixtures of the same molar ratio between standard HAp and t-ZrO2 powders. This plot illustrates that the hardness gradually increases with the treatment temperature and this has the linear relationship with increase in the volume fraction of t-ZrO_2. When temperature is 500 °C, the hardness reaches to about 8.0 GPa, and this value is about 1.6 times higher than that of pure HAp.[17)]

FESEM images of HAp films formed by MAO and HZC films formed by subsequent CVD treatment are respectively presented in Fig. 3(a), (b). The HAp films consist of HAp nanocrystals with average size of 50~60 nm. The HZC samples treated at 500 °C show formation of ZrO_2 nanoparticles (~500 nm in diameter) and nanofibers (~50-80 nm in diameter and ~2-3 μm in length) in the matrix of HAp. As shown in Fig. 3, the nanowires and nanofibers were produced at the surface of HAp. These structures were not identified below 350 °C. Instead, the only spherical nanoparticles of ZrO_2 were distributed. When considering the morphological variation from FESEM images, it seems that some t-ZrO_2 nanoparticles changed their shapes into nanofibers by networking each other. And, again, some nanofibers modified their features in straight form due to the thermal energy. There have been many reports related to these phenomena. When some materials suffer the enough heat or pressure, they tend to grow a certain direction because of their specific crystallographic orientations. Based on this, it is probable that the high crystalline t-ZrO_2 ceramics were formed at the surface of HAp, and thus these ceramics could improve the mechanical properties of HZCs films

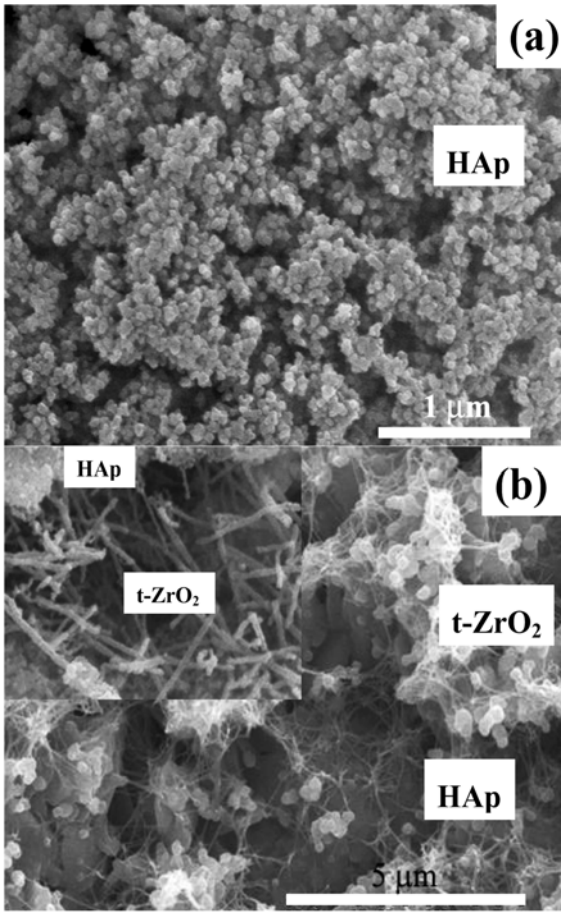

Fig. 3. Field emission scanning electron microscopy (FESEM) images of (a) nanocrystalline HAp films formed by MAO and (b) HZC films formed at 500 °C for 30 min. Inset is a blown-up image of ZrO_2 nanofibers.

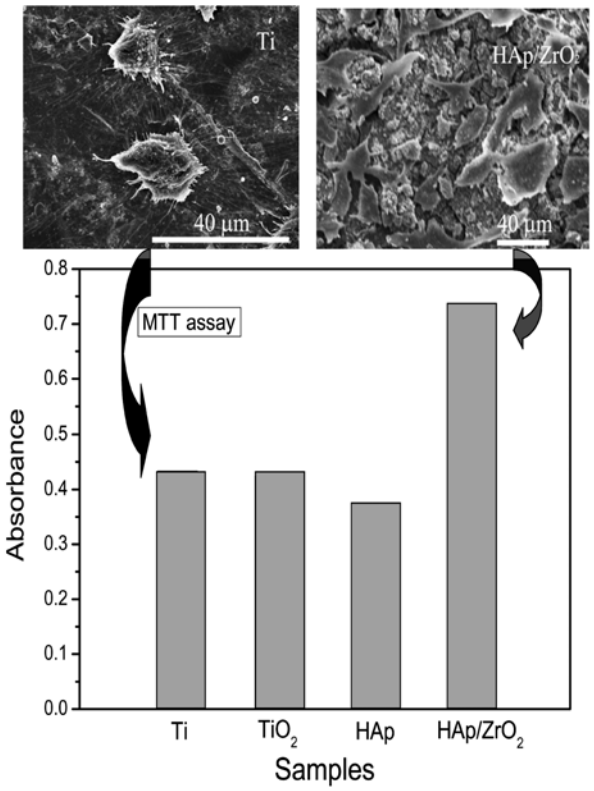

Fig. 4. The mean values of MTT ((3-(4,5-dimethythiazol-2-yl)-2,5-diphenyltetrazolium bromide, 5 mg/ml) assay on pure Ti, MAO TiO_2, MAO HAp, and HZC. Absorbance of dyes was measured at a wavelength of 540 nm via UV-spectrophotometry. FESEM images of MG63 cells proliferated on Ti and HAp-ZrO_2 are also presented.

as shown in Fig. 2.

Fig. 4 shows the comparison in the cell proliferation of different samples. When the cells were cultured on the anatase TiO_2 formed by MAO treatment, the cells exhibited the similar proliferation rate to the pure Ti. As explained above, HAp has strong biocompatibility with a living body, so that coating with HAp was expected to give early cell response. However, contrary to expectation, HAp-coated samples show low absorbance characteristics. In our previous research, it was suggested that all the samples showed the formation of spherical-shape HAp nanoparticles with the size distribution of 50-100 nm as shown in Fig. 3(a)[22] The circumstances can give a disadvantageous effect to the proliferation of cells. The surface consisting of nanoscale particulate materials is not a favorable place for cells having micrometer scale size to proliferate. Probably due to modified morphologies by formation of nanofibers, the ZrO_2-treated HAp films can provides the sites for the cell growth. The ZrO_2 nanofiber structure could provide a nest for the cell attachment and proliferation. This allows HAp to do its intrinsic role of bioactivity and finally cell proliferation rate was improved compared to Ti and TiO_2 samples. FESEM was employed in order to identify the attachment and proliferation of the cells as shown Fig. 4. The number of cells attached to the surface HZC films was larger compared to that of HZC films. In addition, the size of cells grown on the HZCs group was approximately 25-50 μm, while that of the others was 15-25 μm. These results are in good agreement with the MTT test results.

4. Conclusions

High-crystallinity HAp/ZrO_2 composite (HZC) bioceramic films were synthesized on Ti through MAO followed by CVD procedure. Well distributed t-ZrO_2 nanoparticles and nanofibers were formed in the matrix of HAp. Secondary phases such as TCP and TTCP were not detected in the ZrO_2 samples treated at high temperature. Due to the contribution of t-ZrO_2, hardness of the HZC films was improved. The result of cell culturing showed that HZC films have strong affinity with cells. Based on the above investigations, it is possible to find the optimal condition of HZC composites for real applications by controlling the treatment time and temperature. By virtue of the improved mechanical and biological properties, HZC bioceramic films can be widely used for load-bearing and wearing parts in orthopedic and dental prosthesis applications.

Acknowledgement

This work was International Collaboration Research & Development Program through Industry-University Collaboration Consortium by SMBA of Korea in 2008.

References

1. Y. Z. Yang and J. L. Ong, J. Biomed. Mater. Res., **64**, 509(2003).
2. M. M. -Hukovic, E. Tkalcec, A. Kwoka and J. Piljac, Surface Coat. Technol., **165**, 40(2003).
3. X. Nie, A. Leyland, A. Matthews, J. C. Jiang and E. I. Meletis, J. Biomed. Mater. Res., **57**, 612(2001).
4. L. L. Hench and J Wilson, Science, **226**, 630(1984).
5. P. Ducheyne, W. Van Raemdonck, J. C. Heughebaert and M. Heughebaert, Biomater., **7**, 97(1986).
6. T. Kokubo, H. M. Kim and M. Kawashita, Biomater., **24**, 2161(2003).
7. P. Ducheyne, S. Radin, M. Heughebaert and J. C. Heughebaert, Biomater., **11**, 244(1990).
8. M. Svehla, P. Morberg, B. Zicat, W. Bruce, D. Sonnabend and W. R. Walsh, J. Biomed. Mater. Res., **51**, 15(2000).
9. Y. M. Sung, Y. K. Shin, Y. W. Song, A. I. Mamaev and V. A. Mamaeva, Crystal Growth Des., **5**, 29 (2005).
10. P. A. Ramires, A. Romito, F. Cosentino and E. Milella, Biomater., **22**, 1467(2001).
11. Y. Han, J. F. Sun and X. Huang, Electrochem. Commun., **10**, 510 (2008).
12. T. Kokubo, S. Ito, Z. T. Hayashi, S. Sakka, T. Kitsugi and T. Yamamuro, J. Biomed. Mater. Res., **24**, 331(1990).
13. W. Holand, W. Vogel, K. Naumann and J. Gummel, J. Biomed. Mater. Res., **19**, 303(1985)
14. A. Clifford and R. Hill, J. Non-Cryst. Sol., **196**, 346(1996).
15. W. Holand, J. Non-Cryst. Sol., **219**, 192(1997).
16. B. Y. Cjou, E. Chang, S. Y. Ya and J. M. Chen, J. Am. Ceram. Soc., **85**, 661(2002).
17. Y. M. Sung, Y. K. Shin and J. J. Ryu, Nanotechnology, **18**, 065602(2007).
18. L. M. Sun, C. C. Berndt, K. A. Gross and A. Kucuk, J. Biomed. Mater. Res., **58**, 570(2001).
19. Y. C. Yang and E. Chang, Biomater., **22**, 1827(2001).
20. X. Nie, A. Leyland and A. Matthew, Surf. Coat. Technol., **125**, 407(2000).
21. L. H. Li, Y. M. Kong, H. W. Kim, H. E. Kim, S. J. Heo and J. Y. Koak, Biomater., **25**, 2867(2004).
22. M. S. Kim, J. J. Ryu and Y. M. Sung, Electrochem. Commun., **9**, 1886(2007).
23. W. H. Song, Y. K. Jun, Y. Han and S. H. Hong, Biomater., **25**, 3341(2004).
24. R. H. J. Hannik, P. M. Kelly and B. C. Muddle, J. Am. Ceram. Soc., **83**, 461(2000).